Intermediate Report Munich, 30 October 2005

Quantitative evaluation of regional precipitation forecasts using multi-dimensional remote sensing observations (QUEST)

Nicole van Lipzig[1], Felix Ament, Susanne Crewell, Wenchieh Yen
Meteorological Institute, Munich University (MIM)

Monika Pfeifer, George Craig, Martin Hagen
Institute of Atmospheric Physics (DLR)

Marc Schröder, Jürgen Fischer
Institute for Space Sciences, Free University of Berlin (FUB)

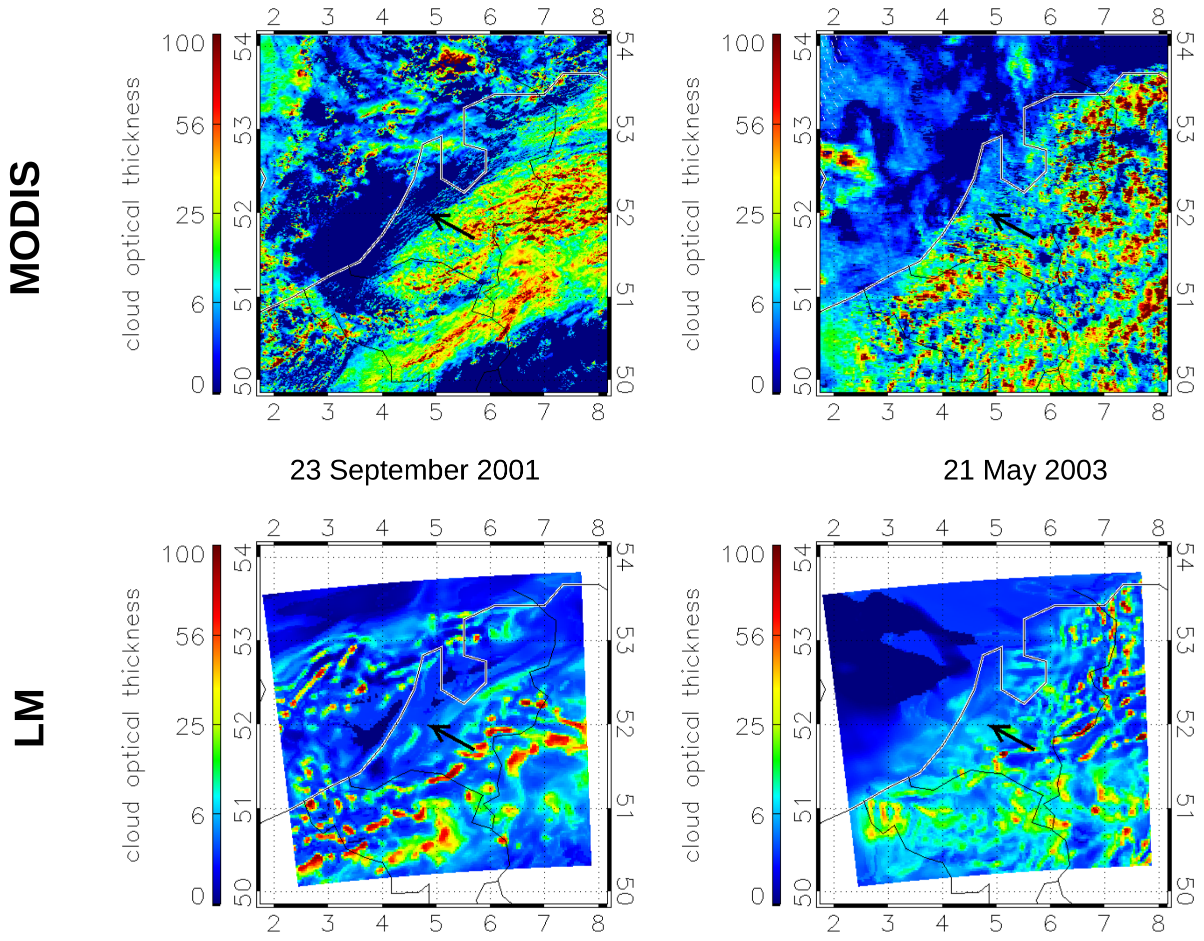

[1] Scientists whose names are underlined were directly funded by DFG; Nicole van Lipzig 1 July 2004 to 30 September 2005; Felix Ament 1 October 2005 – 30 June 2006.

1. Introduction

In order to get insight in the ability of an atmospheric model to simulate the correct surface precipitation, it is of importance to understand the processes leading to formation of clouds and conversion of cloud water and ice into precipitation. Due to the complexity of atmospheric processes it is of utmost importance to observe the atmospheric state as complete as possible. This requires multi-dimensional remote sensing data since they are the only mean to observe the spatial-temporal distribution of water in all its phases.

Within the Schwerpunktprogramm (SPP) of the Deutsche Forschungsgemeinschaft (DFG) the project “Quantitative evaluation of regional precipitation forecasts using multi-dimensional remote sensing observations” (**QUEST**) addresses this po[2]int. The work presented here demonstrates the status after a project duration of about 16 months. In our study active and passive remote sensing instruments both from ground and satellite have been used. Apart from the classical method for model evaluation (“observation-to-model approach”) we have also used the “model-to-observation approach”. The latter method is applied since the remote sensing measurement process involves complex interactions between radiation, the atmosphere (gases, aerosols and hydrometeors) and the surface. As a consequence the determination of model variables from the observations (retrieval) is not straightforward. From a known atmospheric state, the remotely sensed signal calculated with a forward operator (“model-to-observation approach”) is much more accurate. Therefore the comparison of the remotely sensed signal calculated with a forward operator and corresponding remote sensing observations is preferred above a comparison of directly simulated and retrieved atmospheric properties.

To illustrate the type of measurements that we have used within QUEST, Figure 1 shows the temporal development of vertical hydrometeor distribution at Cabauw, the Netherlands. These products have been derived using the Integrated Profiling Technique (IPT; Löhnert et al. 2004). The IPT uses information from various sources (cloud radar, microwave radiometer, lidar-ceilometer, radiosonde, ground-level in-situ measurements) together with error estimates for the derived quantities. It is the first time that the IPT-method is used for the purpose of model evaluation.

In the morning of the selected day (23 September 2001), a stratocumulus field was extending from near-surface to about 1 km height (Figure 1). In the afternoon, the cloud deck broke up, the cloud base moved up and shallow cumuli developed. The Lokal-Modell (LM) forecast shows a patchy structure in Figure 1c, indicating that for this day the lifetime of clouds is underestimated. Moreover, instantaneous in-cloud values of Liquid Water Content (LWC) are much larger than observed. This example provides a first impression of one of the case studies performed within QUEST so far. Apart from profile measurements, 2D and 3D cloud and precipitation fields from satellite and radar were considered to for example investigate whether differences between model and measurements are related to a shift in space or a phasing error in the model. Details can be found in the recently submitted publications by Van Lipzig et al. [2005] and Schröder et al. [2005].

The methods (Sections 4 and 5.1) that we have developed within QUEST are not necessarily routinely applied, but explore the representation of atmospheric processes in the model using conventional and emerging data sources. By using such refined methods, physical consistency is investigated and the model skill of a single variable is of lesser importance. The ultimate goals of QUEST are to study:

Front cover: Cloud optical thickness for 23 September 2001 (left panels) and 21 May 2003 (right panels) derived from MODerate resolution Imaging Spectrometer (MODIS) (upper panels) and simulated with the Lokal Modell using a grid spacing of 2.8 km (lower panels). While the satellite data strongly reflect the stratiform and convective nature of the 2 different cases considered, the model do not show such a strong contast of the two case but rather reveal strong similarities.

i) the systematic errors in the precipitation forecasts of the Lokal Modell (LM) using a grid spacing of 2.8 km,

ii) the typical conditions in which these systematic errors can be most clearly detected and

iii) the relation between correct cloud forecasts and correct precipitation forecasts. Having found situations where the precipitation is wrong, we look for correlated errors in cloud and water vapour to see, whether we can trace the precipitation errors back through the water cycle.

To reach our goals, the work during the first phase of the SPP was stratified into four different tasks, which are the overall co-ordination (WP 1), the organisation of the needed data (WP 2), the tool development (WP 3 and WP 4), and the evaluation (WP 5 and WP 6). An evaluation of the LM for a period of several months (long-term evaluation; LTE; WP 6), enables the identification of systematic biases in this model. As a first step, case studies (WP 5) have been performed in order to see whether there are problems that can be solved easily in the model and to help us in developing a strategy and tools for the LTE (van Lipzig et al., 2004). The LTE will focus on the General Observation Period (GOP) [Crewell et al., 2005] which will be conducted in the 2^{nd} phase of the SPP in 2007.

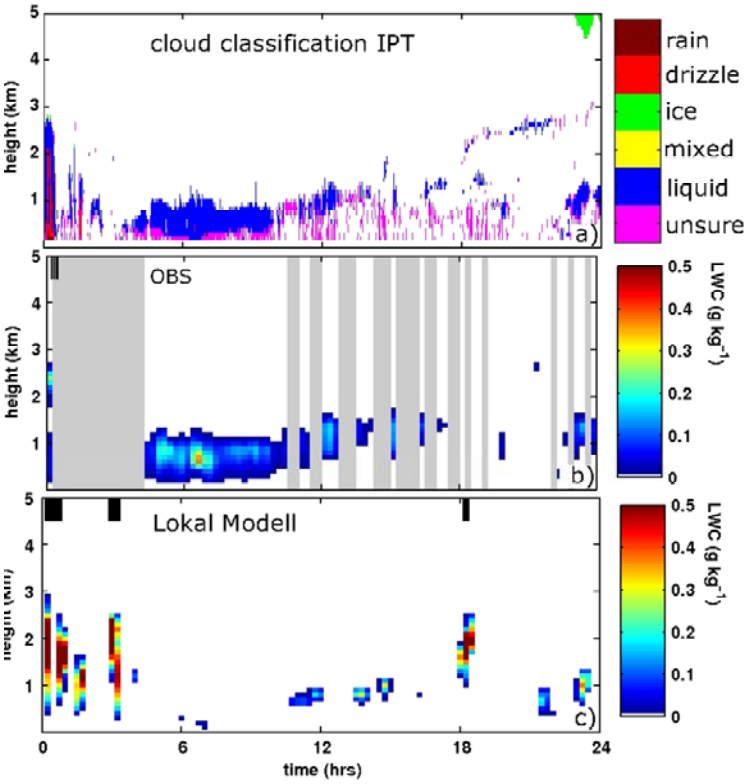

Figure 1. a) Cloud classifications and b) liquid water content (LWC) (g kg^{-1}) in the lowest 5 km of the atmosphere during 23 September 2001 as derived from measurements with the Integrated Profiling Technique (IPT) together with c) output of the Lokal-Modell (LM) at 2.8 km grid spacing. The gray bar in b) indicates the time when no information was available during more than 90% of the interval considered due to failure of one of the instruments or due to an inconsistency between the different instruments. The black bar in the upper part of the graphs indicates the occurrence of precipitation.

It should be noted that QUEST has set up close co-operations with other projects in the SPP which deal with the verification of model forecasts, namely VERIPREC (Mainz), STAMPF (Berlin) and the preparation of the field experiment (Hohenheim/Karlsruhe) resulting in a joint SPP report [Van Lipzig et al., 2005b].

2. Observation data base

The observations used in this study cover vertical (at reference stations), horizontal (from satellite) and three-dimensional (from radar) distributions of water vapour, clouds and precipitation, including all hydrometeors currently used in LM, namely, cloud water, cloud ice and precipitation in the form of water, snow and graupel (Table 1; Figure 2.). An overview about the remote sensing principles of water vapour and clouds can be found in Crewell [2005].

Table 1: Overview of the measurements and products that have been used within the first phase of QUEST.

Satellite remote sensing products	**Satellite remote sensing instruments**	**In-situ instruments**	**Radar**	**Additional Ground based remote sensing**
Cloud mask	Meteosat Second Generation	Rain gauge data	DLR polari-metric radar	Microwave radiometer
Integrated water vapour	MODIS	Radiosonde soundings	DWD weather radars	Lidar
Cloud optical thickness			KNMI cloud radar	
Cloud top pressure				
Liquid water path				

Satellite remote sensing observations utilised in this study were carried out with the MODerate resolution Imaging Spectrometer (MODIS) onboard the U.S (spatial resolution of 0.25 – 1 km). Terra satellite. Terra flies over central Europe 1-2 times a day with overpass times around 10:30 UTC. Furthemore, FUB has its own receiving station for the Spinning Enhanced Visible and Infrared Imager (SEVIRI) / Meteosat Second Generation (MSG). The full disc and all spectral channels (11 channels between 0.6 and 13.4 microns and a high resolution channel with 3 km resolution over Europe) are stored every 15 minutes with a spatial resolution of around 5 km over Europe. The calibrated satellite data are processed automatically to provide higher-order products (e.g. cloud optical thickness). The output of the near real time (NRT) processor is displayed via internet: http://wew.met.fu-berlin.de/nrt. The advantages of satellite observations are the high temporal and spatial resolution, the large coverage, and the fast operational availability.

Clouds are generally characterised by higher reflectances and lower brightness temperature differences than the underlying surface of the Earth. These effects are used to discriminate clear sky from overcast pixels. **Cloud phase** information is determined by utilising differences in the absorption characteristics of liquid and ice water. The retrieval of **cloud top pressure** is based on the CO_2 slicing method and utilises the correlation between absorption intensity and cloud top pressure. The retrieval of **cloud optical thickness** (τ) and cloud droplet **effective radius** (r_{eff}) relies on observations at a non-absorbing channel and a channel affected by liquid water and ice. At non-absorbing channels the reflected intensity is a function of τ. The algorithm separates between τ of liquid water and ice clouds, utilising the cloud phase information. The channels in the near-infrared are affected by absorption of liquid water and allow the retrieval of r_{eff}. The satellite measures r_{eff} of the cloud top and no information is available from layers below. The MODIS products are accessible via internet (Distributed Active Archive Center, DAAC: http://daac.gsfc.nasa.gov). The MOD05 and MOD06 products are described by King et al. (1997) and references therein as well as Menzel et al. (2002) and provide the above products which usually have a spatial resolution of 1 km. The MSG products rely on similar principles, and we started the development of a retrieval algorithm for τ and r_{eff} within QUEST (Section 4.2.1).

Ground-based weather radar observations provide information on precipitation with high spatial and temporal distribution. However, quantitative precipitation estimation (QPE) from radar is still an ongoing research area due to the difficulty in relating the radar reflectivity (sixth moment of the drop size distribution) measured at a certain altitude and distance from the radar to rain rate at the ground. Furthermore, radar calibration, artificial backscattering (clutter), refraction changes, and attenuation contribute to the error sources. Generally, the accuracy decreases with the distance from radar. A number of products is available from the radar network of the Deutscher Wetterdienst (DWD) [Yen et al., 2005]. In addition, we analysed data from the Dutch radar network.

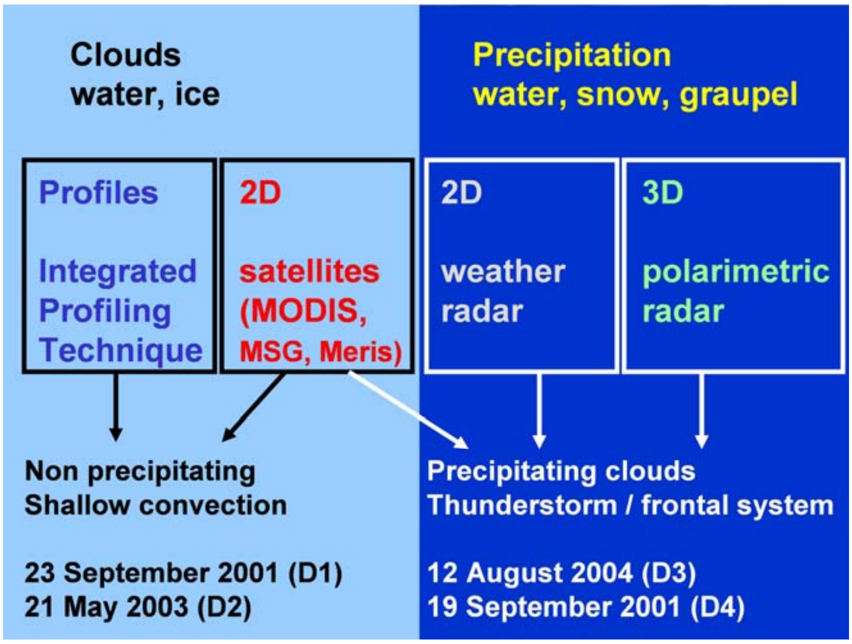

Figure 2. Instruments used for the QUEST case studies. Both clouds and precipitation have been studied including all hydrometeors currently used in Lokal-Modell.

The **DLR polarimetric doppler radar POLDIRAD** is capable of controlling the polarisation of the transmitted wave for each pulse as well as receiving selected polarisation states for the return of each pulse. This in contrast to conventional radar, which can only measure the power of the backscatter signal, a polarimetric radar Hydrometeors, especially in the solid phase, show a high variability in shape, falling behaviour and density depending on their origin in the cloud and the related temperature, super saturation, updraft velocities, etc. Differently polarised radiation, therefore, will be backscattered differently by the various hydrometeor types. The combined information of different polarimetric quantities together with the height of the melting layer allows the classification of the hydrometeor type within the radar volume (Höller et al., 1994). Using this additional information, improved quantitative rain estimates in comparison to conventional radar systems can be obtained and important insights into cloud microphysics are provided. POLDIRAD does not measure operationally. Therefore, this data is only used for selected case studies so far. In the future polarimetric radar will become operational in Germany (Hohenpeissenberg) and other countries although probably with a reduced set of quantities. Furthermore, POLDIRAD will be a key instrument in the upcoming SPP field experiment and the development of the polarimetric model tool should prove beneficial in the future.

At **reference stations** we have applied the Integrated Profiling Technique (IPT; Löhnert et al., 2004), which gives optimal estimates of profiles of LWC, specific humidity (q) and temperature (T). The IPT uses information from various sources (cloud radar, microwave radiometer, lidar-ceilometer, radiosonde, ground-level in-situ measurements). In addition, IPT provides error estimates for the derived quantities. The **cloud radar** has the capability to identify the vertical structure of clouds in the atmosphere, including the detection of cloud top and number of cloud layers but information on LWC is limited. Reflectance from non-meteorological targets (e.g. insects, plant debris) or drizzle with negligible LWC below the cloud base can obscure the signal. Therefore a lidar-ceilometer is used, which is capable to detect the cloud base with an accuracy of 30 m. The **microwave radiometer** is one of the most accurate methods to derive the vertical integral of LWC, namely the Liquid Water Path (LWP) (Westwater, 1987). By comparing atmospheric brightness temperatures at two frequencies, LWP and Integrated Water Vapor (IWV) can be derived simultaneously from the microwave radiometer measurements. In this study, a 'state-of-the-art' microwave profiler with 22 channels was used (the Microwave Radiometer for Cloud Cartography MICCY; Crewell et al., 2001), with a temporal resolution of 1 s and an accuracy of 15 g m^{-2}. During rainfall, the radiometer signal is inaccurate due to wetting of the antenna or radome. Therefore, periods with precipitation are excluded when using these instruments for model evaluation (gray bars in Figure 1).

3. Forecast data base

In preparation for the long-term model evaluation, selected hindcast cases have been performed with the Lokal-Modell (LM) at MIM and DLR. These hindcast cases were:

- **D1**: 23 September 2001: low-level clouds in the morning transferring into shallow cumulus in the early afternoon in the Netherlands
- **D2**: 21 May 2003: two cloud layers during daytime with shallow cumulus and stratocumulus in the Netherlands
- **D3**: 12 August 2004: strong thunderstorm over southern Germany
- **D4**: 19 September 2001: frontal precipitation in the Netherlands

Three different domains have been used. For a comparison with measurements from the Dutch station Cabauw (D1, D2) and KNMI C-Band radar (D4), the model domain covers the Netherlands with 161x161 grid points. Through cooperation with Laboratoire d'Aérologie (LA), GKSS, the Dutch (KNMI) and the Swedish (SMHI) weather services model predictions with the Méso-NH, MM5, RACMO and RCA models were performed for D1 and D2 [van Lipzig et al., 2005a and Schröder et al., 2005]. For the integrations over Germany (D3 and D4), a relatively large area has been chosen including Lindenberg and Cabauw. The model domain is similar, but not identical to the Lokal-Modell-Kürzestfrist (LMK) which is in development at DWD. For the comparisons with the polarimetric radar a smaller domain with 100x100 grid points centered over Munich Airport was used.

A grid spacing of 2.8 km has been used, which is identical to the resolution of LMK. The reason for using this resolution is that the model resolves the process of deep convection and that therefore a parameterisation of deep convection is not needed in the model. In addition, radar data form an important source for the evaluation of the model. On a resolution coarser than 2.8 km, many of the features detected by the radar cannot be resolved. For the different cases, sensitivity studies have been performed in which prognostic equations for different hydrometeors are included. In addition, a sensitivity integration with the shallow convection scheme has been performed. More detailed information on the integrations can be found in Table 2.

For the LTE we are currently using Testsuites performed by the LMK group from DWD, namely Testsuite 2.2b for August 2004 and Testsuite 2.2c for July 2004. Output of these Testsuites are:

- standard GRIB fields, which are saved every hour and are stored in the DWD databank, accessible for all SPP-project scientists.

- additional 2D GRIB fields, which are saved every 15 minutes and stored at FUB and MIM. These additional fields are especially interesting for the comparison with satellite measurements.

Table 2: Overview of the integrations. Described are the time period considered (T_{per}), the institute at which the integration was performed (inst), the model version, the hydrometeors used in the integration (CW Cloud Water; CI Cloud Ice; RW Rain Water; SN Snow; GR Graupel), number of points in x- and y-direction (N_{hor}), number of levels in the vertical (N_{lev}), domain which is covered (domain), initial conditions (ini), lateral boundary conditions (lat), Spin-up time (T_{su}).

T_{per}	23 September 2001; 21 May 2003; 19 September 2001	12 August 2004; 19 September 2001	12 August 2004
inst	MIM	MIM	DLR
model	LM version 3.9	LM version 3.9	LM version 3.15
Hydro	CW, CI, RW, SN	CW, CI, RW, SN	CW, CI, RW, SN, GR
N_{hor}	161 x 161	328 x 378	100x100
N_{lev}	35	35	40
domain	The Netherlands, with the station Cabauw in the center of the model domain	Similar to the operation LMK domain (covering Germany)	smaller domain centered over Munich
ini	LM operational at Δx=7 km	LM operational at Δx=7 km	GME
lat	LM operational at Δx=7 km	LM operational at Δx=7 km	GME
T_{su}	12 hours	12 hours	6 hours

4. Tool development

4.1 Radar simulator

Within WP 3, the polarimetric radar forward operator SynPolRad (Synthetic polarimetric radar, Pfeifer et al., 2004) has been developed (Figure 3). SynPolRad transforms the model output into radar variables as if operating a synthetic polarimetric radar in the model domain. In a first step the electromagnetic

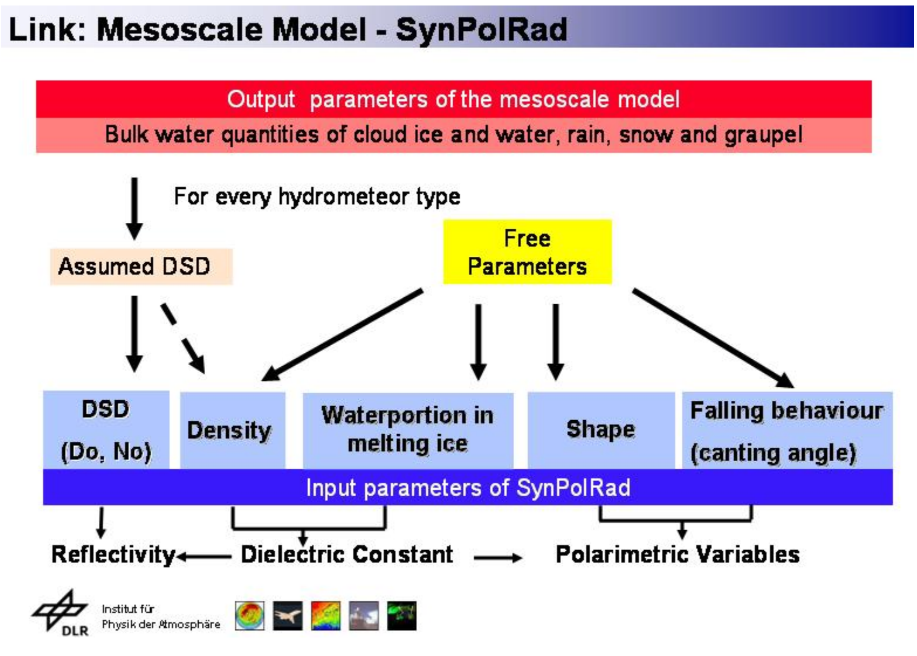

Figure 3. Systematic description of the Radar Simulator SynPolRad.

interactions of the radar beam with the hydrometeors are computed at every model grid point and in a second step the propagation of the radar beam in the model domain is calculated, including consideration of the beam attenuation and refraction depending on the meteorological conditions. For this, SynPolRad combines two existing codes - the conventional radar forward operator RSM (Haase and Crewell, 2000) which models the propagation and attenuation of the radar beam within the model domain and the T-Matrix code (Bringi et al., 1986) to calculate the polarimetric backscatter and the attenuation of the ensemble of hydrometeors within a model grid box. The resulting synthetic parameters are then directly comparable to POLDIRAD measurements. So far, besides reflectivity and specific attenuation, the differential reflectivity ZDR and the linear depolarization ratio LDR are simulated. These quantities are also used for the hydrometeor classification after Höller et al. (1994) allowing a direct comparison of simulated and measured hydrometeor type.

4.2 Tools for comparison with satellite observations

4.2.1 Retrieval of cloud microphysical properties from MSG-SEVIRI observations

We started to develop an algorithm that is capable to retrieve τ, r_{eff}, and LWP from SEVIRI observations in the visible and near-infrared. The inverse problem is solved with an artificial neural network. The input of the network has been composed by the output of sophisticated radiative transfer simulations which have been performed with a wide variety of τ, r_{eff}, surface albedo, and viewing geometry as input. The algorithm is valid for single layer and plane-parallel geometry. Until the end of the first phase of QUEST the set of radiative transfer simulations will be expanded to increase the applicability of the retrieval scheme.

4.2.2 Patchiness

We newly introduced the patchiness parameters in order to compare the structure of cloud cover scenes by a single parameter (Schröder et al., 2005). The degree of patchiness increases with increasing number of overcast and clear sky areas (N_{cld} and N_{free}, respectively). In order to identify a single connected cloud (clear sky) area an eight-(four-)connected neighbour algorithm is applied. Each connected area is labelled with a unique area index which is also used to estimate histograms of the size of cloud areas. The patchiness is characterised by two parameters: The first parameter gives the overall patchiness of the cloud mask and is defined as $p1 = (N_{cld} + N_{free})/n$, with n being the total number of grid cells. Maximum patchiness is achieved, when the cloud mask appears as a chess board. The second parameter assigns a qualitative attribute to $p1$ and is determined as the normalised difference between N_{cld} and N_{free} $p2 = (N_{cld} - N_{free})/n$. If $p2$ is positive (negative), overcast (clear sky) areas contribute most to the patchy appearance of the cloud mask. The patchiness parameters turned out to be a useful extension of standard evaluation approaches (Schröder et al., 2005) and are expected to contribute to an evaluation of existing and future turbulence schemes.

4.2.3 Aggregation of cloud optical thickness with different spatial resolutions

We decided to compare cloud optical thickness, and not LWP, because the reliability of the retrieval of τ is expected to be larger than for a retrieval of LWP from satellite remote sensing observations. We propose to estimate the average (or effective) cloud optical thickness from the transmission (T) according to $T = \exp(-\tau/\mu)$ (μ being the cosine of the sun zenith angle). The transmission T provides the link to radiative transfer, and we aggregate τ by (with i being a spatial grid cell index):

$$\tau = -\mu \ln\left(1/N \sum_i \exp(-\tau_i/\mu_i)\right).$$

This equation is used to aggregate MODIS cloud optical thickness onto the model grid. After aggregation the equation is used to determine the domain average cloud optical thickness.

LM has fractional cloud cover for each of its layers. The fractional cloud cover indirectly requires a spatial average of overlapping clear sky and overcast parts of the layers. We integrate as follows:

$$\tau_{cloud} = -\mu \ln\left(\prod_j \left(1 - b_j + b_j \exp(-\tau_j/\mu)\right)\right),$$

with j being a layer index. τ_{cloud} is subsequently converted into an effective cloud optical thickness of the grid box utilising columnar cloud cover (more details in Schröder et al., 2005). Scene and domain averages of satellite and model are determined independently of each other, i.e. no overlap of clouds is required between satellite and model. In this way, misinterpretations due to missing cloud areas in the model output are avoided. The above equations offer a general approach for a comparison of high resolution cloud optical thickness retrieved from satellite observations to corresponding output from atmosperic models with lower resolutions.

4.2.4 Tracking of convective cells

We developed a tracking algorithm that can be applied to rain rate observations and simulations as well as to brightness temperature (BT) observations and simulations. Convective cells are defined by applying a threshold to either rain rates or BT observations, and each cell is assigned a unique area index. The systems are tracked by finding the minimum in the difference of area and position between two successive images. It allows a statistical analysis of the path, growth rate, life time, and origin of convective cells. In addition, the temporal evolution of cloud properties of individual cells can be monitored. Future development will address uncertainties related to merging and splitting.

5. Model evaluation

5.1 Process studies

5.1.1 BALTEX-Bridge Campaign cases

We have used data from two intensive cloud measurement campaigns for the evaluation of LM. These campaigns BBC (BALTEX Bridge Campaigns; August and September 2001) and BBC2 (May 2003) were held in the Netherlands [Crewell et al., 2004] around a central experimental facility at Cabauw (51°58' N, 4°55' E). Two days with shallow convection were selected from the BBC dataset, namely 23 September 2001 (D1) and 21 May 2003 (D2), for the **WMO international cloud modeling workshop**, held in Hamburg in 2004 (Crewell et al., 2004b). Apart from the evaluation of the short-term cloud and precipitation forecasts of the LM, we also evaluated five other European models using this dataset [Van Lipzig et al., 2005 and Schröder et al., 2005]. The novel aspect of this evaluation was the vertical distribution of clouds (Figure 1) which was put into context with boundary layer development and spatial structures from satellite and radar observations.

The main result is that the LM underestimates the lifetime of clouds, but at the same time overestimates the liquid water content. This is reflected in an overestimation of the temporal variability in the time versus height plots of LWC and an overestimation of the temporal variations in LWP (Figure 1 and Figure 4). A measure for temporal variations is the **autocorrelation function** (Ra) as defined by Lumley and Panofsky (1964):

$$Ra(\Delta t) = \frac{\overline{LWP(t)LWP(t+\Delta t)}}{\overline{LWP^2}}$$

where $\overline{LWP(t)LWP(t+\Delta t)}$ is the autocovariance using a time separation of Δt and $\overline{LWP^2}$ is the variance. The time separation (Δt) at which the signal goes to zero is an indication for the time period for which clouds typically exist and thus an indication for the lifetime of clouds. To obtain a quantitative measure for the intermittency of LWP and the lifetime of clouds, the autocorrelation function was integrated over time separations (Δt) up to 1.25 hr [Van Lipzig et al., 2005a]. This integral is referred to as Ri. The LM value for Ri (15 min) is much lower than the measured value (34 min) for D1 (Figure 4c). A comparison between modelled vertical velocity and LWC in LM indicates that the temporal evolution of LWC is closely related to updrafts and downdrafts in the model. The model might alias sub-grid scale convective motions to the resolved scale. A quantitative evaluation of the vertical velocity is unfortunately not possible since no measurements for that quantity are available. Note that with the cloud radar the ensemble weighted fall velocity of the droplets can be measured, but not the vertical velocity of the air. A new method suggested by Protat et al. [2003] might improve that situation in the future.

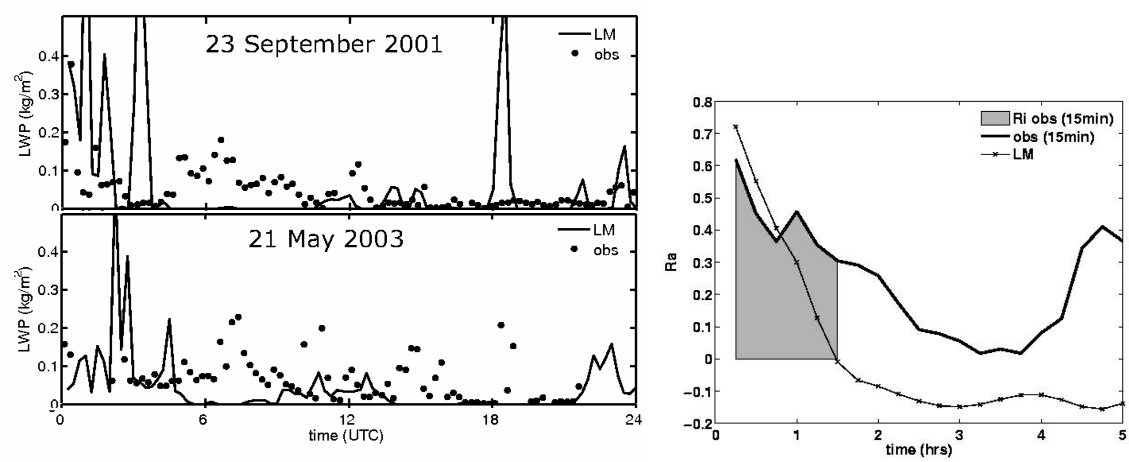

Figure 4. Liquid water path during a) 23 September 2001 and b) 21 May 2003 as observed by the Microwave Radiometer for Cloud Cartography MICCY (symbols) together with the LM output for the Cabauw grid box (solid line). c) The autocorrelation function (Ra), defined as the autocovariance using a time separation of Δt divided by the variance. Ra is plotted as a function of Δt for the observed LWP time series using an aggregation time of 15 min (thick solid line) and LM (thin solid line). The grey area shows the integral of Ra over time separations Δt up to 1.25 hr, which is introduced as a measure for the intermittency of LWP and the lifetime of clouds. This integral is referred to as Ri.

The model predictions were also compared to satellite observations [Schröder et al., 2005] using the methods (single cloud parameters; optical depth) presented in section 4. LM underestimates the **patchiness** of the 2D cloud cover relative to the MODIS cloud cover on D1 and D2, though LM, in agreement with MODIS, reveals larger patchiness on D2 than on D1, revealing the convective nature of D2. The underestimation is consistent with a simultaneous underestimation of the frequency of occurrence of small cloud areas. A comparison of **cloud optical thickness** (see front cover and Schröder et al., 2005) shows structural differences: The stratiform cloud on D1 could not be reproduced by LM, which exhibits isolated medium sized clouds with large τ, and though a convective tendency can be deduced on D2, it underestimates small scale cloud structure, also showing medium sized clouds with large τ. Figure 5 shows a **histogram** of τ on D1 and confirms the visual impressions. The overestimation at small cloud optical thicknesses leads to an overestimation of domain average cloud optical thickness. The underestimation and overestimation of the frequency of occurrence at intermediate and large τ is consistent with the correlation of large LWC with strong updrafts. Furthermore, these results indicate that the underestimation of the lifetime of clouds is not due to advection of too small cloud systems, but rather due to an overestimation of the variability in the vertical velocity. We also found that the amount of high-level clouds is overestimated in LM relative to MODIS on D1 and D2. In Schröder et al. (2005) we demonstrate that this is most likely related to the inability of MODIS to detect thin cirrus clouds. If a threshold of 0.7 g m^{-2} is applied to remove thin ice clouds, the agreement between LM and MODIS largely improves.

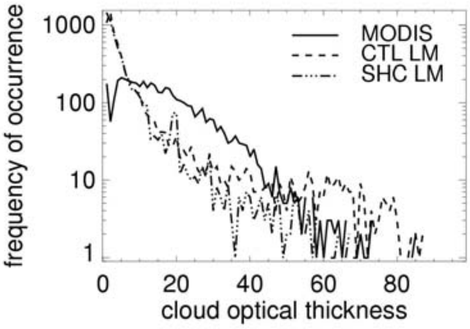

Figure 5. Histogram of cloud optical thickness from MODIS and the CTL and SHC runs of LM on D1.

Apart from the cloud structures, the **inversion in LM is too weak** and too close to the surface. Mixing of moisture to higher atmospheric levels is underestimated, which is reflected in an overestimation of the vertical gradient in the specific humidity. The occurrence of precipitation in the model is overestimated for these two cases, in other words, the model seems to produce **too much drizzle**, which might be related to the parameterization of autoconversion rates. However, a long-term evaluation is needed to confirm this preliminary result. The introduction of the shallow convection does indeed lead to an increase in mixing of moisture in the troposphere, but the vertical gradient is still overestimated.

5.1.2 Exemplary thunderstorm case (12 August 2004)

The case study for 12 August 2004 (D3), when a front moved over Germany and heavy thunderstorms occurred in southern Germany, is useful to illustrate the methods used in QUEST. The clouds and precipitation are studied using the DWD radar international composite, the POLDIRAD reflectivity, and MSG derived cloud cover and brightness temperature. As an illustration, Figure 6 shows the situation at 18:00 UTC when a heavy thunderstorm was present in the Munich region. As can be seen on the top row, the strong thunderstorm in the region of Munich is not represented by the LM using the full model domain over Germany. Sensitivity tests were performed using a smaller domain and it was found that the thunderstorm is better represented, when a small domain over the Munich area excluding the Alps was chosen (second row left panel). This sensitivity run indicates that during this day the foehn effect in the high-resolution domain is overestimated when the Alps are included. Comparison between LM and MSG derived cloud cover has been performed (Figure 6 bottom row). Figure 7a shows the temporal evolution of the mean cloud cover over Germany both from LM and from MSG. It can be seen that the timing of the high clouds related to the front is about two hours early for this day. This apparent time shift is due to high level clouds: If clouds with IWP<0.7 g m^{-2} (with simultaneously low LWP values) are removed, it becomes evident that the time shift is caused by high thin ice clouds which are not present in the observations. In addition, the model has a too low occurrence of small cloud fields (Figure 7b). A comparison between modeled precipitation and precipitation derived from the DWD weather radar (not shown) shows that the timing of the precipitation related to the front is too late. In addition, there is a latitudinal dependence of the delay of the front: In the South, the delay is larger than in the North.

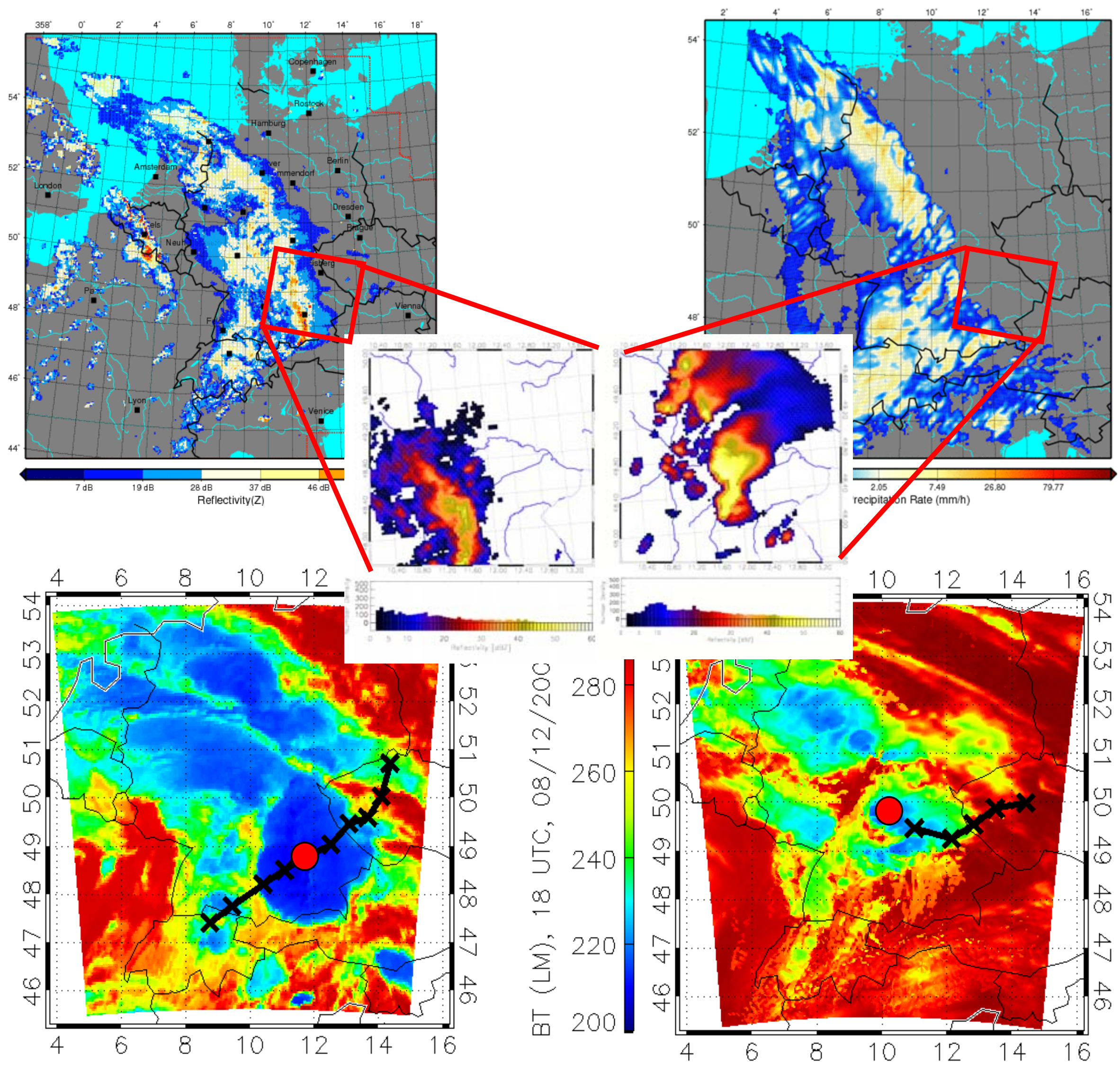

Figure 6. Top row: Radar reflectivity (Z) composite (left) of the frontal system moving over Germany on 12 August 2004 at 18 UTC and corresponding LM precipitation (R) forecast (right). The forecast was started at 12 UTC on the previous day using a grid spacing of 2.8 km. Colour schemes are matched to represent standard Z-R relation. Middle row: Polarimetric radar observations by POLDIRAD (left) in southern Germany and the radar simulation from SynPolRad based on LM forecast (right) both on 12 August 2004 at 18 UTC. The reflectivity histogram is plotted at the bottom. Bottom row. Brightness temperature at 10.8 µm observed by Meteosat Second Generation (left) and calculated by SynSat from LM forecast (right) both on 12 August 2004 at 18 UTC. The black line shows the track of the most intense (coldest) part of the precipitation system from 14 to 23 UTC (left). The track in the left panel starts later in the evening (19 UTC). The red dot indicates the current position at 18 UTC.

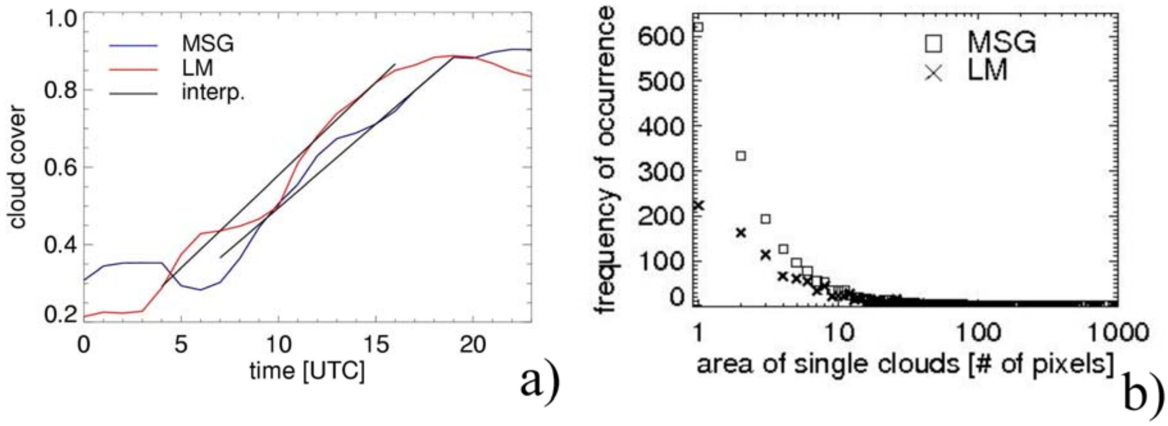

Figure 7. a) Cloud cover over Germany as measured by Meteosat Second Generation (blue line) and as modeled by LM (2.8 km horizontal resolution, red line) on 12 August 2004. b) Frequency distribution of cloud size as measured by Meteosat Second Generation (squares) and as modeled by LM (crosses) for 12 August 2004.

Figure 6 (lowest left panel) shows the path of the largest convective cell on D3, determined by the tracking algorithm applied to BT observations from MSG. In Schröder et al. (2005a) a reasonable agreement between the path determined on the basis of BT and rain rate observations is demonstrated while the path of the largest rain area in LM is shifted to the North. The cloud top height retrieval shows average values around 196 hPa in the POLDIRAD domain at 19:30 UTC, in consistence with the large vertical extent found in POLDIRAD observations (Figure 9). The minimum BT is close to 205 K in MSG observations, with an average of 220 K. The average BT determined by the newly implemented radiation scheme (Testsuite 2.2) is 264 K, with a minimum of 215 K. The difference to MSG is caused by a shift of the cirrus shield to the North-West and an underestimation in size. Figure 6 (right lower panel) shows that the track of the cell in the vicinity of Munich is similar to the track in the observations but convective activity starts too late in this area. Furthermore, we found that the region of largest underestimation of integrated water vapour at 11 UTC is located at a position which will become the center of the cell around 19 UTC. The identified differences need to be verified by analysis of long-term data sets which will be accomplished in the near future.

Together with the front, strong convective activity was observed with POLDIRAD, operated at Oberpfaffenhofen. This observation is compared to the synthetic reflectivity calculated with SynPolRad [Pfeifer et al, 2004] of the LM integrations. The model underestimates the high reflectivities that were measured by the DLR polarimetric radar for the thunderstorm in Munich. This indicates that the intensity of the convective event is underestimated by this LM integration. Additional integrations were made for a smaller domain of 100 x 100 grid points (see Table 2 for more details). These integrations turned out to much better represent the convective event in the Oberpfaffenhofen region.

Figure 8 shows a vertical cross section through the LM model domain for synthetic reflectivity, ZDR and LDR. Two cores of heavy precipitation can be recognized in all three variables with the highest values in reflectivity reaching 50 dBZ within the rain region. ZDR which is a measure of oblateness of particles has the highest values in the cores of heavy rain in well agreement with the expectations and observations. The same is true for LDR, which is a measure for tumbling ice hydrometeors, having the highest values in the graupel region as well as in the strong rain, where large, oblate drops tend to tumble. So far only LDR and ZDR were considered for evaluation, but also rhoHV and KDP are available through the T-Matrix, but the corresponding measurements from Poldirad are not yet available.

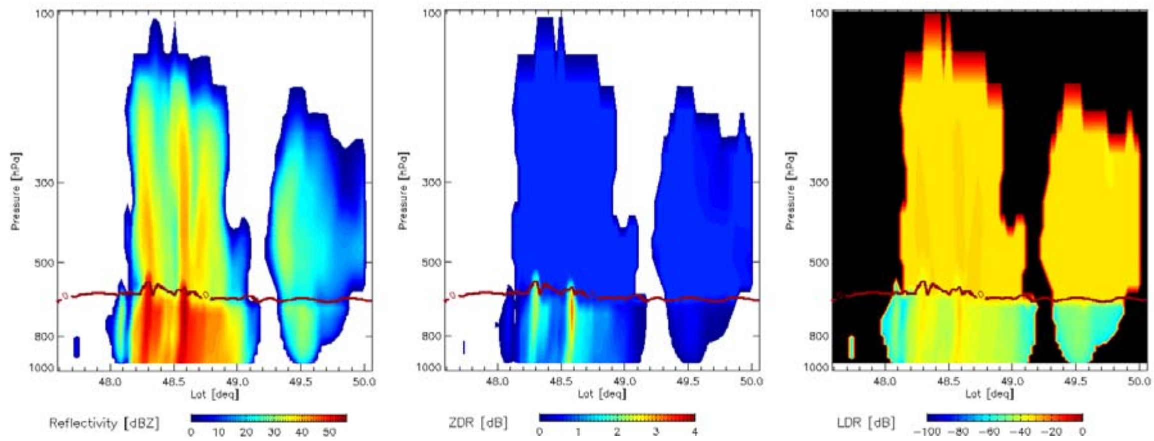

Figure 8.: Vertical cross section of reflectivity (left), differential reflectivity ZDR (center) and linear depolarisation ratio LDR (right)at 12 August 2004 17:00 UTC.

5.2 Sensitivity studies

From the process studies (Section 5.1) several model deficiencies were identified. First of all, the model derived synthetic reflectivities show a strong brightband signal, which is not measured by POLDIRAD. This phenomenon is likely to be caused by the absence of graupel as a prognostic variable. Therefore a sensitivity integration, with graupel included as a prognostic variable, has been performed. Secondly, a grid spacing of 3 km is too coarse to resolve the shallow convective clouds. Therefore a sensitivity integration, in which shallow convection is parametrised, has been done. These two sensitivity studies are discussed below.

5.2.1 Implementation of the graupel scheme

For 12 August 2004, the model was run in the operational mode including the 2-component precipitation scheme with prognostic rain and snow and the research mode including the 3-component scheme with prognostic rain, snow and graupel. Comparing the RHI of POLDIRAD (Figure 9) and the synthetic RHI (Figure 10) it can be seen that the radar scan shows more structure, with a stratiform region on the left featuring relatively weak reflectivities of 10 dBZ and two cores of strong precipitation related to graupel and hail attaining maximum reflectivities of up to 55 dBZ. Because of their high density, hail and graupel fall rapidly to the ground showing the typical hail signal throughout the whole vertical extent of the cloud. The maximum synthetic reflectivity calculated with the 2-component scheme reaches even higher values, but is organised in a bright band structure, which cannot be seen in the actual radar image. In the region of the melting layer, a water coat evolves around the melting snow crystal increasing the dielectric constant and therefore the reflectivity massively while the crystal size diminishes very slowly through melting. This process normally becomes visible in radar observations when the precipitation above the 0° isotherme is dominated by very light and therefore slowly falling ice crystals and is a typical feature of stratiform precipitation. Looking at the 3- component scheme including the graupel phase, the brightband has vanished, but still the graupel phase is too light to reach the ground before melting as it can be seen in the Poldirad scan. Because hail and graupel not only contribute to the precipitation at the ground, but also are responsible for the evolution of the typical strong downdroughts and the dynamical structure, the LM will not be able to create realistic thunderstorms before having included heavier species of precipitating ice. The implications for the life cycle of thunderstorms in the LM and the related precipitation at the ground have to be further investigated.

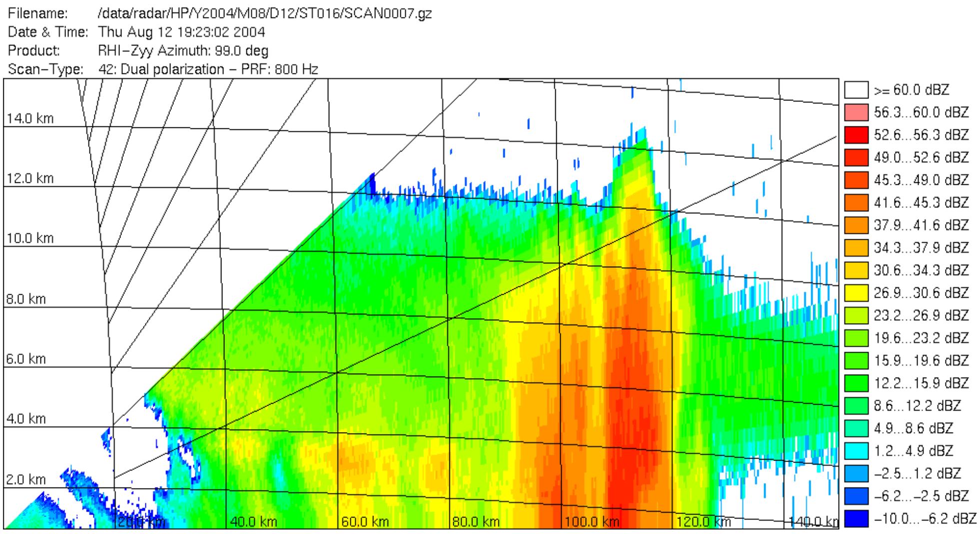

Figure 9. POLDIRAD scan of reflectivity [dBZ] on the 12th of August 2004 showing a vertical cross section (RHI) through a convective system at 19:23 UTC.

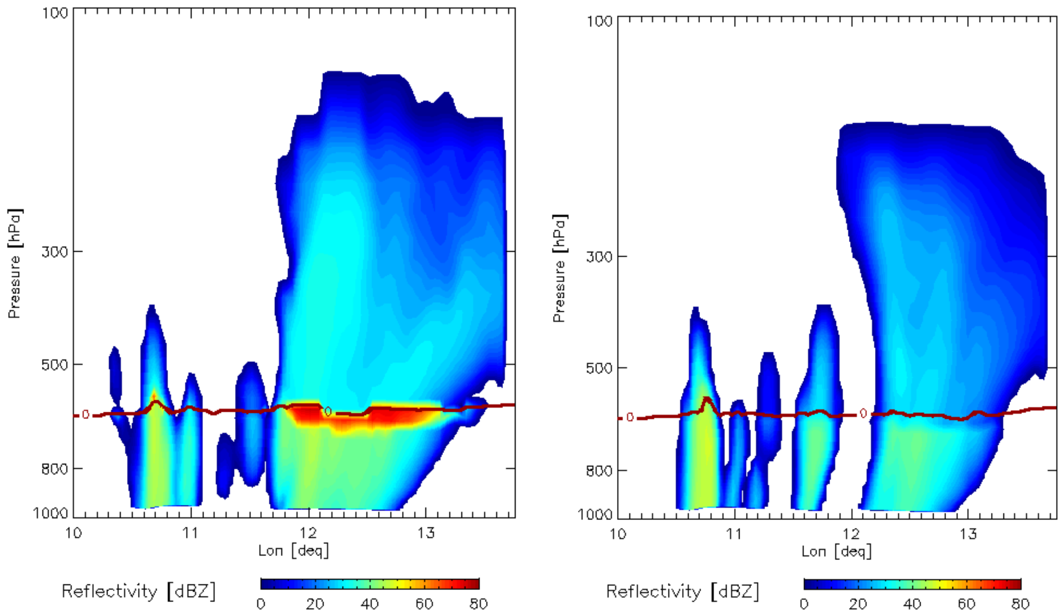

Figure 10. The synthetic reflectivities [dBZ] of a convective system on 12th of August 2004 at 19:00 UTC as simulated by the LM with a horizontal resolution of 2.8 km. In the left figure calculations where done with the 2 component scheme including prognostic rain and snow, and in the right figure with the 3 component scheme including prognostic rain, snow and graupel.

5.2.2 Implementation of the shallow convection scheme

Clearly, a grid spacing of 3 km is too coarse to resolve shallow convective clouds. Indeed from our results in Section 5.1.1 it is obvious that deficiencies exist in representing shallow clouds in the non-hydrostatic models. The models might overestimate the updrafts by aliasing sub-grid scale convective motions to the resolved scale and consequently they overestimate in-cloud LWC. For this reason, we have tested how the implementation of a shallow convection scheme affects the representation of low level clouds. The runs excluding (including) parameterised shallow convection will be referred to as CTL (SHC).

The shallow convection scheme is identical to the deep convection scheme of Tiedtke (1989), but only when P_{SHC} is less than 250 hPa, the tendencies in the model are updated. When the convection is deeper than P_{SHC}, the vertical velocity related to the convective system is assumed to be resolved by the model and convective tendencies from the scheme are ignored. Note that DWD is planning to develop a more sophisticated scheme allowing determination of entrainment and detrainment as diagnostic quantities in terms of Convective Available Potential Energy (CAPE).

Parameterised convection introduces a mechanism to transport heat and moisture to higher atmospheric levels without the necessity of resolved-scale vertical motion. Therefore the inversion is at higher elevation and the potential temperature and specific humidity (q) are found to be more homogeneously distributed in SHC compared to the CTL-integration. This causes a weakening of the resolved-scale updrafts and a decrease in their frequency, which in turn leads to a decrease in the number of clouds and the LWC within the clouds (Figure 11).

For D1, the implementation of SHC does not affect the lifetime of clouds and the implementation of SHC is not solving this problem in LM. The value for Ri decreases from 15 min to 9 min and is still much lower than the measured value (34 min). LWP decreases by as much as 80% on D1 when SHC is switched on, which is related to the weakening of the resolved-scale updrafts in the SHC-integrations. This large sensitivity in the model indicates that, for LWP, the turbulent transport in the models is a crucial factor, a result consistent with the findings of Zhu et al. (2005). For D2 the sensitivity of LWP is much smaller and the mean LWP during the day is identical in CTL and SHC.

Figure 5 presents the histogram of cloud optical thickness related to an implemented shallow convection scheme (SHC). A clear decrease of the frequency of occurrence of large cloud optical thicknesses is found when the shallow convection scheme is implemented. Additionally, an implemented SHC leads to a reduction of total cloud cover and average cloud optical thickness on D1 and D2. Despite the increased agreement at large frequencies of occurrence the changes do not decrease the differences between LM and MODIS (more details to SHC runs in Section 5.2.2).

The gradient in q decreases in SHC and is in better correspondence with the measurements compared to the CTL-integration. In general, model output is sensitive to the implementation of SHC, but except for the q profile a clear improvement in the behaviour is not found when SHC is implemented for the two shallow convection cases D1 and D2 (Van Lipzig et al., 2005; Schröder et al., 2005).

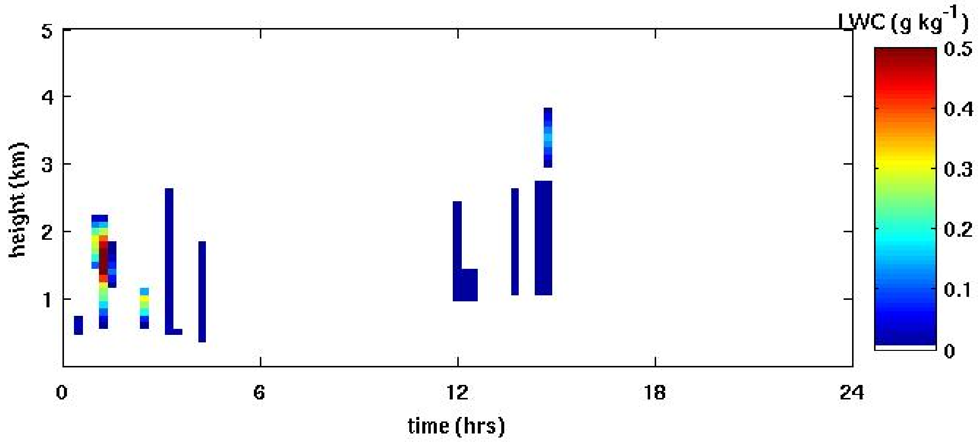

Figure 11. Same as Figure 1c, but with the shallow convection scheme implemented.

5.3 Long-term evaluation

The long-term evaluation (LTE) applies the methods developed in the framework of case studies to longer time series. In the first phase of QUEST, the focus of LTE is on evaluating the LMK TestSuite integrated by DWD (for technical details see also end of Section 3). It is expected that this model has an improved skill to predict extremes of precipitation and the spatial structures of rainfall. The objective of QUEST is to test these hypotheses and to trace back model deficiencies throughout the entire hydrological cycle. Work on the LTE has been started after the analysis of case studies was finished and final results are not available at the time this report is issued. Nonetheless, the example presented in the following illustrates the potential of LTE and what kind of results can be expected by the end of the first phase of QUEST.

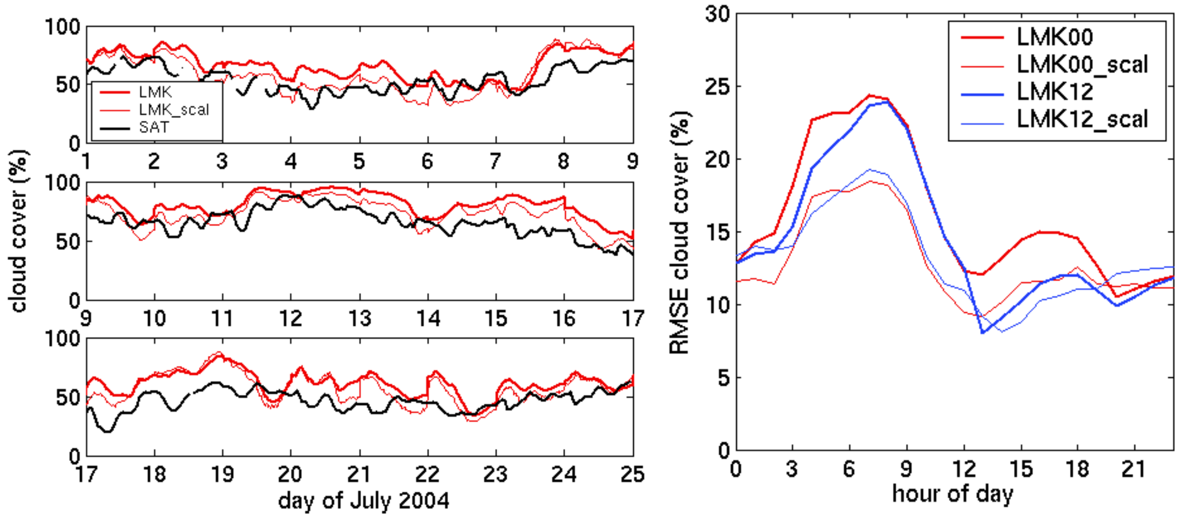

Figure 12. Left: Time series of mean cloud cover retrieved from MSG observations and modelled by LMK (24h forecast starting at 00 UTC) averaged over the LMK domain. Right: Daily cycle of root mean square area in modelled domain mean cloud cover. Additionally, the results of the LMK forecasts starting at 12 UTC are displayed in blue. Thin, coloured lines indicate the modelled cloud cover if only grid-scale clouds are taken into account.

Figure 12 shows a comparison of cloud cover retrieved from MSG observations and modelled by the LMK TestSuite 2.2c in terms of an average over the LMK domain (excluding the boundary zone of the model, which is artificially affected by the boundary conditions). In the left panel, it can be seen, that the model represents the overall evolution of cloud cover quite well. Nevertheless significant deviations occur at different temporal scales, which are partly not detectable by case studies: There are episodes lasting a couple of days at which the amount of cloud cover is largely overestimated (e.g. 15 - 19 July) and periods with a much better agreement (e.g. 10-11 July or 23-24 July). Correlating these temporal error patterns to errors in other quantities, like IWV or precipitation, as well as identifying the weather conditions which are connected to such periods gives insight into the underlying mechanism. Another approach to explain model problems is to use the LTE as a tool for case study selection and to identify days which are well suited for investigating certain model problems.

In general, the evaluation of the cloud cover reveals that the LMK tends to overestimate the cloud cover. This error is most pronounced during the morning (see Figure 12, right panel), but can be reduced by taking only the grid-scale clouds into account. This is an indication to reconsider the subgrid-scale cloud scheme, which was initially developed for coarse scale models with a resolution in the order of more than 10 km and might not be suitable for LMK anymore. Ignoring model predicted thin ice clouds, which are hardly detectable by the MSG retrieval, might even further reduce the positive BIAS of simulated cloud cover.

Since the LMK is operated as a lumped ensemble (i.e. temporally overlapping model simulations started at different times of the day) it is possible to analyse the effect of data assimilation: By reinitializing the model at 00 UTC (LMK00), the error in predicted cloud cover is not changed whereas reinitializing the model at 12 UTC (LMK12) results in a significant error reductions. It is most likely that prescribing analysis data at 12 UTC effectively cures systematic errors which have been accumulated throughout the morning. Extending the LTE to a larger set of variables, which will be conducted in the remaining time of the first phase of QUEST, will give answers to such open questions.

6. Summary

Several **tools have been developed** within the first phase of QUEST, namely i) the polarimetric foreward operator SynPolRad, ii) algorithms to retrieve microphysical properties from satellite observations and iii) the development of several quantitative measures for model evaluation. Examples of the latter are the pathiness parameter, which gives a quantitative measure for the structure of cloud cover scenes, algorithms for tracking of convective cells and a measure based on the autocorrelation function, which gives a quantitative measure for the lifetime of clouds.

Observations from two intensive cloud measurement campaigns have been used to evaluate five regional models including the Lokal-Modell (LM) at 2.8 km grid spacing. Two shallow convection cases were selected for the **WMO international cloud modeling workshop**, held in Hamburg 2004. The novel aspect of this evaluation was the vertical distribution of clouds which was put into context with the boundary-layer development and the spatial cloud structures from satellite and radar observations. The comparison of cloud optical thickness was found very useful to judge the performance of shallow convection schemes. While the satellite data strongly reflect the stratiform and convective nature of the two cases considered, the different high resolution models do not show such a strong contrast between the two cases but rather reveal strong similarities. The underestimation of the lifetime of clouds, which was found in LM, is not due to advection of too small cloud systems; it is rather caused by an overestimation of the variability in the vertical velocity.

All QUEST tools which were developed in the first phase, were applied to several **heavy precipitation cases**. A case with frontal precipitation moving over Germany, with heavy thunderstorms in Southern Germany (12 August 2004) points to several model deficits that need to be tested in a long-term evaluation. First of all, the forecasted high pre-frontal clouds appeared too early, whereas the precipitation related to the front was slightly delayed in the model. In addition, by using polarimetric radar observations it was found that two model prognostic falling hydrometeors (precipitation and snow) are insufficient to obtain a realistic structure of the convective cell. In especially an unrealistic brightband is found in the LM synthetic radar image.

The impact of two **model improvements** has been tested namely the implementation of graupel as a prognostic variable in LM and the implementation of a shallow convection parametrisation scheme. The comparison between model and the DLR polarimetric doppler radar (POLDIRAD) improves when graupel is included, but the graupel is still too light to reach the ground before melting. The parametrisation of shallow convection leads to more homogeneous temperature and specific humidity boundary-layer profiles, causing a weakening of the resolved-scale updrafts and a decrease in their frequency. Consequently, parametrised shallow convection leads to a reduction of total cloud cover and average cloud optical thickness. For the cases considered, no clear improvement in model forecast was found when shallow convection was parametrised.

In collaboration with the DWD, **a long-term evaluation** of the Lokal-Modell-Kürzestfrist (LMK) testsuites is currently underway. From these preliminary results it is shown that LMK represents the evolution of cloud cover well with a tendency to overestimate it. Many variables will be considered together to get a better understanding of the model shortcomings. Extensive use will be made of data becoming available from the **General Observation Period (GOP)** in 2007.

References

Bringi, V.N., R. M. Rasmussen, J. Vivekanandan, 1986. Multiparameter Radar measurements in Colorado convective Storms. Part {I}: Graupel Melting Studies. Journal of the Atmospheric Sciences, 42, 22, 2545-2563

Crewell, S., Czekala, H., Löhnert, U., Simmer, C., Rose, T., Zimmermann, R., Zimmermann, R., 2001. Microwave Radiometer for Cloud Carthography: A 22-channel ground-based microwave radiometer for atmospheric research. Radio Science 36, 621-638.

Crewell, S., Simmer, C., Bloemink, H., Feijt, A., García, S., Jolivet, D., Krasnov, O., van Lammeren, A., Löhnert, U., van Meijgaard, E., Meywerk, J., Pfeilsticker, K., Quante, M., Schmidt, S., Schröder, M., Scholl, T., Trautmann, T., Venema, V., Wendisch, M., Willén, U., 2004a. The BALTEX Bridge Campaign: An integrated approach for a better understanding of clouds. Bull. Amer. Meteor. Soc. 85(10), 1565-1584, doi: 10.1175/BAMS-85-10-1565.

Crewell, S., van Lipzig, N.P.M., Ament, F., Carqué, G., Chaboureau, J.-P., Grützun, V., Guo, X., Kuba, N., Leporini, M., Matthias, V., van Meijgaard, E., Quante, M., Schröder, M., Willén, U., Yen, W., 2004b. Shallow convection cases from the Baltex BRIDGE Campaigns: Results from the WMO international cloud modeling workshop 2004. Report for WMO workshop.

Crewell, S., 2005: Hydrological applications of remote sensing: Atmospheric states and fluxes Water vapor and clouds (passive/active techniques), Encyclopedia of Hydrological Sciences, Wiley & Sons (in press).

Haase, G, Crewell, S, 2000. Simulation of radar reflectivities using a mesoscale weather forecast model. Water resources Research, 36, 8, 2221-2231

Höller, H., Bringi, V.N., Hubbert, J., Hagen, M., and P.F. Meischner, 1994: Life Cycle and precipitation formation in a hybrid-type hailstorm revealed by polarimetric and Doppler radar-measurements. *J. Atmos. Sci.*, **51**, 2500-2522.

King, M.D., Tsay, S.C., Platnick, S.E., Wang, M., Liou, K.-N., 1997. Cloud retrieval algorithms for MODIS: Optical thickness, effective particle radius, and thermodynamic phase. Algorithm Theoretical Basis Document ATBD-MOD-05, NASA Goddard Space Flight Center.

Löhnert, U., Crewell, S., Simmer, C., 2004. An integrated approach towards retrieving physically consistent profiles of temperature, humidity, and cloud liquid water. J. Appl. Meteorol. 43(9), 1295–1307.

Lumley, J.L., H.A. Panofsky. The Structure of Atmospheric Turbulence. New York: Interscience Publishers, 1964.

Menzel, W.P., Bryan, B.A., Strabala, K.I., Frey, R.A., 2002. Cloud top properties and cloud phase - Algorithm Theoretical Basis Document. ATBD-MOD-04, NASA Goddard Space Flight Center.

Pfeifer, M., G. Craig, M. Hagen, C. Keil: A polarimetric radar forward operator, Proc. Third European Conference on Radar in Meteorology and Hydrology (ERAD), Visby, Sweden, 494-498, 2004.

Protat, A., Lemaitre, Y., Bouniol, D., 2003. Terminal fall velocity and the FASTEX cyclones. Quart. Jour. Roy. Meteorol. Soc., 129 (590), 1513-1535.

Schröder, M., N.P.M. van Lipzig, J. Fischer, 2005a. New methods for the evaluation of atmospheric models with satellite remote sensing observations applied to two cases from the BALTEX Bridge Campaigns In: Geophysical Research Abstracts, General Assembly of the European Geophysical Union, Vienna, Austria. (EGU05-A-08407) CD-ROM.

Schröder, M., van Lipzig, N. P. M., Ament, F., Chaboureau, J.P., Crewell, S., Fischer, J., Matthias, V., van Meijgaard, E., Walther, A., Willén., U., 2005.. Comparison of model predicted low-level cloud parameters with satellite remote sensing observations during the BALTEX Bridge Campaigns. Atm. Res. (submitted).

Tiedtke, M., 1989. A comprehensive mass flux scheme for cumulus parameterization in large-scale models. Mon. Wea. Rev. 117 (8), 1779-1800.

Van Lipzig, N.P.M., Schröder, M., Crewell, S., Ament F., Chaboureau J.-P., Löhnert, U., Matthias, V., van Meijgaard, E., Quante, M., Willén, U., Yen, W., 2005a. Comparison of model predicted low-level cloud parameters with observations from the BALTEX-Bridge Campaign. Atm. Res. (submitted).

Van Lipzig, N.P.M., Wernli, H., Crewell, S., Gantner, L., Behrendt, A., 2005. Synthesis of preliminary results of SPP verification projects. Newsletter des SPP 'Quantitative Niederschlagsvorhersage' - 26.08.2005 - Nr. 1/2005b.

Van Lipzig, N.P.M., Pfeifer, M., Schröder, M., Ament, F., Craig, G., Crewell, C., Fischer, J., Hagen, M., Yen, W., 2004. Strategy for the long-term evaluation of the model output from the Lokal Modell. SPP Report.

Westwater, E.R., 1978. The accuracy of water vapor and cloud liquid water determination by dual-frequency ground-based microwave radiometry. Radio Science 13, 677-685.

Zhu, P., Bretherton, C.S., Köhler, M., Cheng, A., Chlond, A., Geng, Q., Austin, P., Golaz, J.-C., Lenderink, G., Lock, A., Stevens, B., 2005: Intercomparison and interpretation of single column model simulations of a nocturnal stratocumulus topped marine boundary layer. Mon. Wea. Rev. (in press).

QUEST-related publications

Crewell, S., N. van Lipzig, W. Yen, J. Fischer, M. Hagen, C. Koziar and M. Schröder: General Observation Period (GOP) 2007, SPP 1167 Colloquium, Bad Honnef, 10-11 März, Poster.

Pfeifer, M., G. Craig, M. Hagen, C. Keil 2004: A polarimetric radar forward operator, Proc. Third European Conference on Radar in Meteorology and Hydrology (ERAD), Visby, Sweden, 494-498.

Pfeifer, M, 2005: Evaluierung der Niederschlagsvorhersage durch polarimetrisches Radar, Mittelungen DMG, 01/2005, ISSN 0177-8501, p.10-12

Pfeifer, M, M. Hagen, C. Keil, 2005: Precipitation forecast evaluation by polarimetric radar. In: Abstracts of the World Weather Research Programme Symposium on Nowcasting and Very Short Range Forecasting, Toulouse, France, p.275

Schröder, M., van Lipzig, N. P. M., Ament, F., Chaboureau, J.P., Crewell, S., Fischer, J., Matthias, V., van Meijgaard, E., Walther, A., Willén., U., 2005.. Comparison of model predicted low-level cloud parameters with satellite remote sensing observations during the BALTEX Bridge Campaigns. Atm. Res. (submitted).

Schröder, M., N.P.M. van Lipzig, J. Fischer, 2005b. New methods for the evaluation of atmospheric models with satellite remote sensing observations applied to two cases from the BALTEX Bridge Campaigns In: Geophysical Research Abstracts, General Assembly of the European Geophysical Union, Vienna, Austria. (EGU05-A-08407) CD-ROM.

Van Lipzig, N.P.M., Schröder, M., Crewell, S., Ament F., Chaboureau J.-P., Löhnert, U., Matthias, V., van Meijgaard, E., Quante, M., Willén, U., Yen, W., 2005a. Comparison of model predicted low-level cloud parameters with observations from the BALTEX-Bridge Campaign. Atm. Res. (submitted).

Van Lipzig, N.P.M., Wernli, H., Crewell, S., Gantner, L., Behrendt, A., 2005b. Synthesis of preliminary results of SPP verification projects. Newsletter des SPP 'Quantitative Niederschlagsvorhersage' - 26.08.2005 - Nr. 1/2005b.

Van Lipzig, N.P.M., S. Crewell, F. Ament, G. Craig, J. Fischer, M. Hagen, M. Pfeifer, M. Schröder, W. Yen, 2005c. Quantitative evaluation of regional precipitation forecasts using multi-dimensional remote sensing observations. In: Abstracts of the 5th international scientific conference on the Global Energy and Water Cycle, Costa Mesa, USA. p. 283.

Van Lipzig, N.P.M, S.Crewell, H.K. Baltink, 2005d. New methods for the evaluation of low-level clouds in atmospheric models using ground-based remote sensing applied to the BALTEX Bridge Campaign cases. In: Geophysical Research Abstracts, General Assembly of the European Geophysical Union, Vienna, Austria. (EGU05-A-09353) CD-ROM.

Yen, W., S. Crewell, N. van Lipzig and J. Seltmann, 2005: DWD Radar Products for Model Evaluation in SPP 1167, SPP 1167 Colloquium, Bad Honnef, 10-11 März, Poster.